

COBEM-2017-1557

SHAPE DISTORTION PREDICTIONS OF CURVED SANDWICH PANELS: A PARAMETRIC STUDY

Olumide Mayowa Makinde

Mechanical Engineering Division, Technological Institute of Aeronautics-ITA
olumidemakinde@yahoo.com

Alfredo Rocha de Faria

Mechanical Engineering Division, Technological Institute of Aeronautics-ITA
arfaria@ita.br

Mauricio Vicente Donadon

Aerospace Engineering Division, Technological Institute of Aeronautics-ITA
donadon@ita.br

Abstract. *The residual stresses that develop during the manufacture of fibre reinforced composite panels lead to shape distortions, which are also known as spring-in. These distortions are a major source of problems for composite manufacturers. Consequently, the ability to effectively and efficiently predict these distortions is always desired. In this paper, process induced shape distortions for various sandwich curved panels was predicted with the aid of the constitutive model originally proposed by Svanberg and Holmberg. The model is implemented as user defined material model within solid elements in ABAQUS. Several factors, which include variation in the radius of curvature, stacking sequence (UD, Cross laminate and Quasi isotropic laminate), fibre volume fraction and percentage of core material used, were considered in the simulations. From the results obtained, a regression-based parametric study was done. Additionally, a stacking sequence modification coefficient was introduced based on statistical analysis of the FEA results. By incorporating this coefficient, the regression-based model can be used to predict the distortions of any stacking sequence investigated. The model was validated against the FEA solutions with relative accuracy. This work provides a platform to develop proactive control techniques for manufacturing curved sandwich composite panels with improved dimensional tolerance for aerospace structures applications.*

Keywords: : Residual stresses, Shape distortions, Spring-in, Composite, Curved Panels

1. INTRODUCTION

Composite sandwich structures with curved geometry finds extensive use in the aerospace and wind-turbine industries. However, the manufacture of these structures is usually accompanied by shape distortions and residual stresses. These shape distortions is the increase/decrease of the external angle of a composite structure after curing, as explained in Fig. (1) and Fig. (2). To obtain accurate composite parts that adhere to the design geometry, composite manufacturer's have resulted to an iterative process, involving the modification of tool profiles after initial trials in order to compensate for shape distortions. This is even more difficult for large, curved sandwich panels used in the wind-turbine blade industry which can be complex due to the disparate constituents (Mahadik and Potter, 2013). These distortions cause difficulties in assembly thereby leading to increased manufacturing costs. On the other hand, the residual stresses in these parts reduces the mechanical strength of these parts. There is therefore an interest in ensuring predictability of shape distortions and residual stresses in the manufacture of these sandwich panels with a view to save costs.

Based on numerous research studies done to understand the development of residual stresses and shape distortions, several factors are known to be responsible for the spring-in phenomenon. These factors are classified as intrinsic or extrinsic factors. Intrinsic factors include, CTE anisotropy, isothermal cure shrinkage of the resin, fiber type and fiber volume fraction. Extrinsic factors include cure schedule, shape and size of the structure, type of mold and tool part interaction among others (Çınar et al., 2014). These factors can also be grouped into two categories: those that cause distortion that is recoverable by reheating (known as thermoelastic spring-in) such as CTE anisotropy and material property gradients and those that form permanent deformation independent of temperature such as cure shrinkage and tool part interaction.

Using Fig. (1), Radford and Rennick (1997) showed that the spring-in angle, $\Delta\theta$, for corner sections can be predicted from geometry and thermal expansion strains by using Eq. (1).

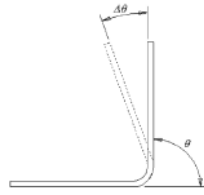


Figure 1: Angle section showing spring-in (Svanberg and Holmberg, 2001)

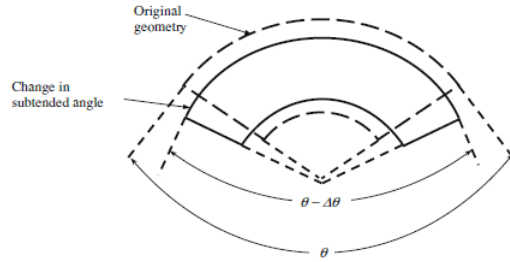


Figure 2: Spring-in of curved panels (Ersoy et al., 2010)

$$\Delta\theta = \theta \left[\frac{\varepsilon_1 - \varepsilon_3}{1 + \varepsilon_3} \right] \approx \theta(\varepsilon_1 - \varepsilon_3) \quad (1)$$

Where ε_1 and ε_3 are the free expansion in the in-plane and through-thickness directions respectively. $\Delta\theta$ is the spring-in angle and θ is the angle surrounded by the bend. Equation (1) shows that the major cause of deformation is the difference between the thermal expansion in the longitudinal direction and through-the-thickness direction of a composite part. The coupling of the non-uniform strains induced by cool-down from cure temperature with a curved geometry cause changes in curvature that account for a large part of the deviation of the final part from the tool geometry. Because the through-the-thickness CTE of composite laminates is almost always greater than that of the in-plane direction, the deformation of an angle section is inwards, hence the name spring-in commonly given to process induced deformations. Additionally, using a simple analytical model described in Eq. (2), Fernlund (2005) captured the effect of the contributions of the sandwich core to the spring-in phenomenon of a composite part.

$$\Delta\theta = \left\{ \theta_0 * \left(\frac{1 + \varepsilon_{\phi s}}{1 + \varepsilon_{rs}} \right) * \left(\frac{1}{1 + \frac{\varepsilon_{rc} - \varepsilon_{rs}}{(1+t_0/c_0)(1+\varepsilon_{rs})}} \right) \right\} \quad (2)$$

Where θ_0 represents the initial angle of the structure, ε_{rc} is the radial strain of the core and ε_{rs} is the radial strain of the skin. Additionally, $\varepsilon_{\phi s}$ is the tangential strain of the skin while t_0 and c_0 are the initial thickness of the skin and initial core thickness respectively. Fernlund concluded that the effect of the core on spring-in is a function of the difference between the through the thickness strains of the core and the skins. If the thermal radial strain of the core was more than that of the skin, then the spring-in would increase and vice versa.

A number of experimental studies to characterize the influence of layup, laminate thickness, cure cycle, tool surface as well as initial geometry on spring-in were conducted by Albert and Fernlund (2002) and Fernlund et al. (2002). Svanberg and Holmberg (2001) demonstrated how the cure schedule affects spring-in. Svanberg and Holmberg (2001) used variations in mould temperature to separate the mechanisms that cause spring-in. Svanberg confirmed that three mechanisms are responsible for the shape distortions: thermal expansion (different in glassy and rubbery state), chemical shrinkage and frozen-in deformations. Twigg et al. (2003) confirmed that a sliding interface condition occurs during the majority of the cure cycle, although, the tool and part sometimes adhere together resulting in high inter-facial shear stresses. The tool-part interaction occurs despite the use of a release agent with the use of a fluoro-ethylene-propylene (FEP) release film at the tool-part interface reducing the effect. Mahadik and Potter (2013) ascertained that the major contributors to thermoelastic spring-in of curved sandwich panels were found to be the thermal expansion and Poisson's ratio of the foam. The study also confirmed the development of resin rich regions on the surface of the panel which also affected the spring-in of the curved sandwich panel.

Several finite element models have also been developed to predict the spring-in experienced in composites. Svanberg and Holmberg (2004a) developed a simplified mechanical constitutive model, in incremental form, which is applicable for

a curing resin or homogenised curing composite. The model captured the mechanisms that were identified in Svanberg and Holmberg (2001) as important for prediction of shape distortions: thermal expansion, chemical shrinkage and recovery of frozen-in deformations. The model was used in Svanberg and Holmberg (2004b) to accurately predict the spring-in of several monolithic composite parts with a good accuracy. The results show that changing the mechanical boundary conditions significantly affects the prediction. In another work, Ersoy et al. (2010) used a two-step FE model to represent the development of stresses during cure process in curved composite parts. The results of the analysis correlated well with experimental results with variances depending on the thickness of the tubes been predicted. Experimental spring-in angles were very close to those predicted for the thicker tubes, and slightly lower for the thinner ones. Other models developed to predict spring-in phenomenon include (Johnston et al., 2001; Kappel et al., 2015; Mezeix et al., 2015)

Dong et al. (2004) used a FEA-based dimension variation model to predict deformations of typical composite structures. Thereafter, a regression-based dimension variation model was developed to provide a quick reference guide for prediction of several shapes. The model helps to provide a quick guide for designers and develop practical and proactive dimension control techniques for composite products. In the same vein, Makinde et al. (2017) extended the parametric analysis of contributing factors to shape distortion in L-Shaped composite structures using the Svanberg model. The study showed that there are some factors whose contributions can not be neglected in the prediction of spring in phenomenon. These factors include stacking sequence, fibre volume fraction and radius of curvature.

In this study, a regression-based parametric study of curved sandwich structures is done using the three-dimensional version of the plane-strain constitutive model originally proposed by Svanberg and Holmberg (2004a). several factors were considered in the parametric study. They include variation in the radius of curvature, stacking sequence (UD, Cross laminate and Quasi isotropic laminate), fibre volume fraction and percentage of core material used. Using the regression-based variation model, the process induced distortions of curved sandwich composite panels can be predicted effectively and efficiently.

The method involves computing the deformation of composite parts using finite element analysis. Thereafter, the deformations of composite structures can be computed using the regression-based model.

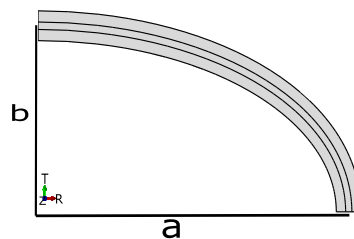


Figure 3: Curved panel showing dimensions, Material regions and Datum Axis

2. FINITE ELEMENT MODELLING

The mechanical constitutive model developed by Svanberg and Holmberg (2004a) has been implemented in ABAQUS as a user subroutine, UMAT Manual (2010) in 4 steps. Details about the constitutive model could be obtained in Svanberg and Holmberg (2004a) while the details about the process followed could be obtained in Makinde et al. (2017).

2.1 Geometry

The sandwich panel was modelled as a quadrant panel with varying radius of curvature as shown in Fig. (3). The thickness of the panel studied was 6mm. Dimension a , which is kept constant throughout the simulations at 50mm, is measured along the major axis while dimension b is measured along the minor axis, is varied from 25mm to 50mm. The panels is divided into 3 regions with the center region representing the core region and the two outer regions representing the skin. The thickness of the skin regions are equal thereby presenting a symmetric laminate. The thickness of the core region is varied as a percentage of the whole thickness from 0% to 75%.

2.2 Material properties

The materials used for modeling of the skin is glass fibre while the material used for the core is divinyl. The material mechanical properties of the skins and the core used are in Tab. 1. The fibre direction coincides with the hoop direction of the geometry. For the skin, the mechanical properties of fibre and matrix laminate (glassy and rubbery state) were calculated using self-consistent-field micro-mechanics obtained from Bogetti et al. (1995) and 3D-laminate theory obtained from Chen and Tsai (1996). Mechanical properties of E-glass fibres were obtained from Kaw (2005) while the

properties of the matrix were obtained from Svanberg and Holmberg (2001). For the core (divinyl cell), the mechanical properties were obtained from Fernlund (2005). The core remains stable even at high temperatures hence there is no rubbery phase or liquid phase in the properties of the core. For the composite skin, the mechanical properties in the liquid phase is assumed to be zero while gelation (X_{gel}) occurs at 34%. The mechanical properties of the core remains the same irrespective of phase. The lay-up sequence studied were for Unidirectional lay-ups $[0]_{ns}$, Cross ply $[0/90]_{ns}$ and Quasi-isotropic $[90/45/-45/0]_{ns}$ lay-ups. Where n is the number of layers above the midplane of the skin. The fibre volume fraction studied was from 45 percent to 55 percent.

Table 1: Mechanical Properties of Glass-Epoxy skin ($V_f = 45\%$) and Di-vinyl Cell Foam Core

Property	Value		Di-vinyl Core	Units
	Rubbery	Glassy		
$E_{11} = E_{22}$	21.2	17.16	138	GPa
E_{33}	7.81	2.13	138	GPa
ν_{12}	0.09	0.0021	0.32	-
$\nu_{13} = \nu_{23}$	0.46	0.86	0.32	-
G_{12}	2.33	2.48e-02	33	GPa
$G_{13} = G_{23}$	2.22	2.48e-02	33	GPa
$\alpha_{11} = \alpha_{22}$	16.09	5.53	3.5e-5	$10e^{-6}/^{\circ}C$
α_{33}	7.13	285.8	3.5e-5	$10e^{-6}/^{\circ}C$
$\beta_{11} = \beta_{22}$	-4.0e-03	-8.55e-05	0	$10e^{-6}/^{\circ}C$
β_{33}	-0.0234	-0.0379	0	$10e^{-6}/^{\circ}C$

2.3 Meshing, Boundary Conditions and Thermal Loading

The mesh and boundary conditions for the curved panels is shown in Fig. (4). The element used is an 8-node linear brick, reduced integration, hourglass control element(C3D8R). One element is used for each ply in the through-the-thickness direction. Multiple elements were used to model the core in the through-the-thickness direction. Nodes between the skins and the core were merged fully, assuming a completely fixed adhesion between the laminate plies.

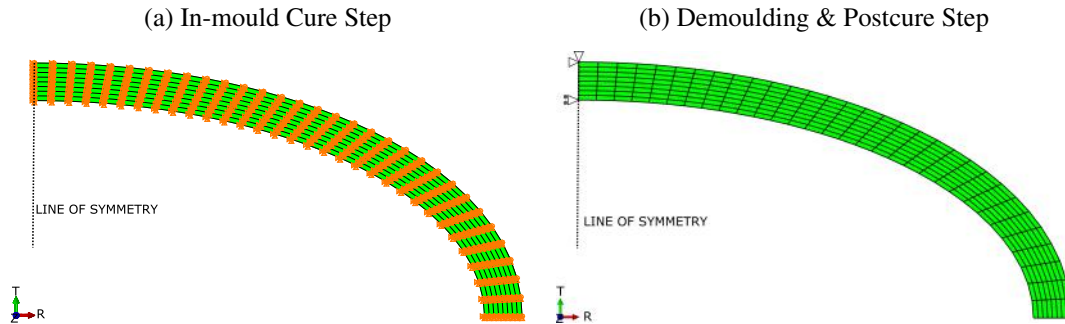


Figure 4: Finite Element Mesh and the Boundary conditions for the curved panels

Two different mechanical boundary conditions have been used in the model. In the first case (in-mould step), the whole part was fully constrained to simulate the in-mould cure phase of curing and to obtain a crude approximation of the constraint from the mould. In the remaining steps (demould and post-cure steps), a boundary condition to prevent rigid body motion was employed. Symmetry boundary conditions was applied along the line of symmetry. Only half of the curved panel is modelled, taking advantage of the symmetry.

A temperature of $80^{\circ}C$ was applied to all nodes to simulate an homogeneous heating of the part in the first step. During this first step, part was fully constrained to simulate the in-mould cure phase of curing. The Tg attained after the first step of in mould cure corresponds to 91 percent degree of cure. After this step, the boundary conditions of the part was changed by removing constraints so that only rigid body motion remains suppressed simulated demoulding. Thereafter, an increment in the temperature up to $120^{\circ}C$ and then cooling down to $20^{\circ}C$.

2.4 Results

Figure. (6a) shows the stress distribution of a curved panel with 50% core while Fig. (6b) shows the deformation of the same curved panel with 50% core. After the simulation, the angular deformation was measured. To measure the value of the angular deformation, the cured tip location was compared with the uncured tip location as shown in Fig. (5).

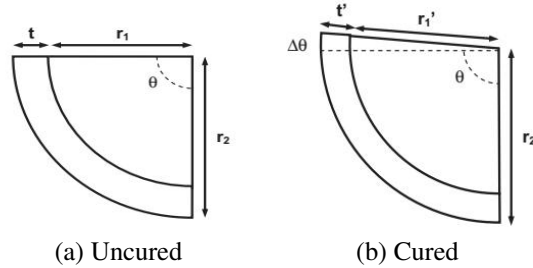


Figure 5: Analytical approximation for change in angle of a curved section Radford and Rennick (2000)

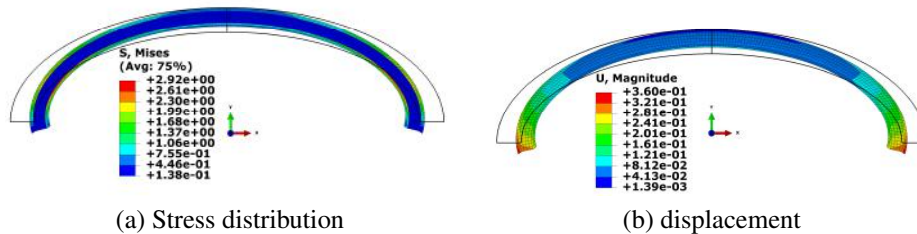


Figure 6: Stress distribution and displacement of a curved panel with 50% core

3. REGRESSION BASED PARAMETRIC MODEL

The study was carried out on curved panels with varying parameters. The parameters include variation of minor axis of the curved panel denoted as a , variation of the Fibre Volume Fraction denoted as V_f , variation of the core percentage denoted as p and stacking sequence. The following paragraphs capture the effect of each parameter on the spring in of curved sandwich panels.

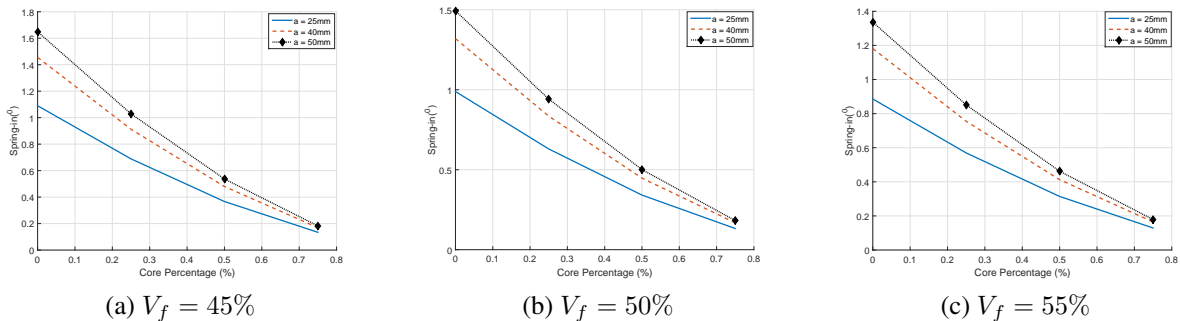


Figure 7: Effect of variation of core percentage on Spring-in

3.1 Effect of Variation of Core Percentage

The results in Fig. (7) and Fig. (8) show that the spring-in angle reduces quasi-linearly as the percentage of the core increases. This phenomenon is expected as the core contributes only to spring-in due to thermal effect. The regression models for the curves in Fig. (7) were developed in Eq. (3).

$$\Delta\theta_{V_f=45\%} = \begin{cases} 1.0485 - 1.2761p & (a = 25\text{mm}) \\ 1.3982 - 1.717p & (a = 40\text{mm}) \\ 1.5828 - 1.9561p & (a = 50\text{mm}) \end{cases} \quad (3a)$$

$$\Delta\theta_{V_f=50\%} = \begin{cases} 0.95175 - 1.1431p & (a = 25\text{mm}) \\ 1.2689 - 1.537p & (a = 40\text{mm}) \\ 1.4358 - 1.75p & (a = 50\text{mm}) \end{cases} \quad (3b)$$

$$\Delta\theta_{V_f=55\%} = \begin{cases} 0.85336 - 1.0101p & (a = 25\text{mm}) \\ 1.1374 - 1.3574p & (a = 40\text{mm}) \\ 1.2864 - 1.5447p & (a = 50\text{mm}) \end{cases} \quad (3c)$$

Based on these equations, the general model to describe the effect of the variation of core percentage on the Spring-in angle is

$$\Delta\theta = \begin{cases} 0.518 + 0.0215a - 0.6004p - 0.0274ap & (V_f = 45\%) \\ 0.4712 + 0.0195a - 0.5401p - 0.0244ap & (V_f = 50\%) \\ 0.4235 + 0.0174a - 0.479p - 0.0215ap & (V_f = 55\%) \end{cases} \quad (4)$$

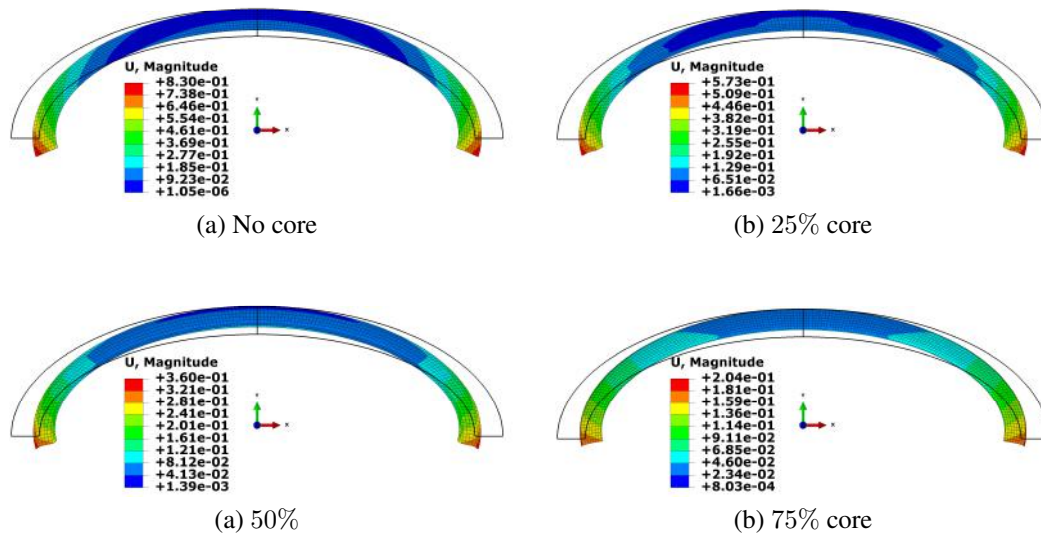


Figure 8: Deformation of curved panels with increase in Core percentage for a = 25mm

3.2 Effect of Variation of Minor Axis

Figure (9) and Fig. (10) show the effect of the variation of the minor axis on Spring-in. The figures show that as the curvature of the part increases, the spring-in angle increases. By examining the curves in Fig. (10), the regression models written in Eq. (5) are obtained.

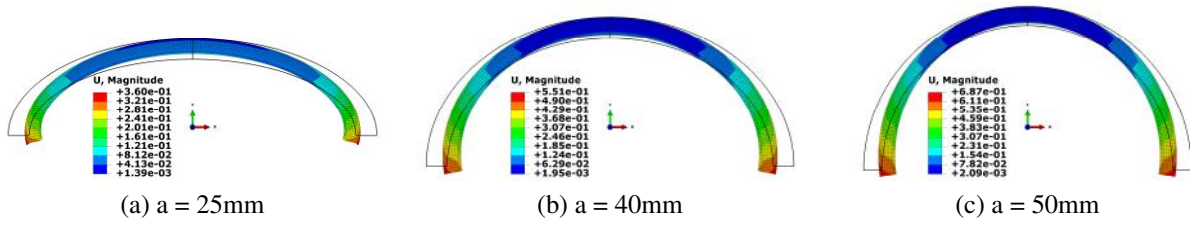


Figure 9: Deformation of curved panels with increase in the minor axis ($V_f = 50\%$)

$$\Delta\theta_{V_f=45\%} = \begin{cases} 0.022499a + 0.5357 & (0\% \text{ core}) \\ 0.013715a + 0.35104 & (25\% \text{ core}) \\ 0.0068625a + 0.19805 & (50\% \text{ core}) \\ 0.0019714a + 0.086357 & (75\% \text{ core}) \end{cases} \quad (5a)$$

$$\Delta\theta_{V_f=50\%} = \begin{cases} 0.020341a + 0.48761 & (0\% \text{ core}) \\ 0.012561a + 0.32064 & (25\% \text{ core}) \\ 0.0064403a + 0.18301 & (50\% \text{ core}) \\ 0.0020197a + 0.08344 & (75\% \text{ core}) \end{cases} \quad (5b)$$

$$\Delta\theta_{V_f=55\%} = \begin{cases} 0.018159a + 0.43851 & (0\% \text{ core}) \\ 0.011361a + 0.28961 & (25\% \text{ core}) \\ 0.0059666a + 0.16749 & (50\% \text{ core}) \\ 0.0020212a + 0.080032 & (75\% \text{ core}) \end{cases} \quad (5c)$$

The regression model that best describe the effects of variation of minor axis on spring-in is Eq. (6)

$$\Delta\theta = \begin{cases} 0.5719 - 0.6004p + 0.0215a - 0.0274ap & (V_f = 45\%) \\ 0.4712 - 0.5401p + 0.0195a - 0.0244ap & (V_f = 50\%) \\ 0.4235 - 0.479a + 0.0174p - 0.0215ap & (V_f = 55\%) \end{cases} \quad (6)$$

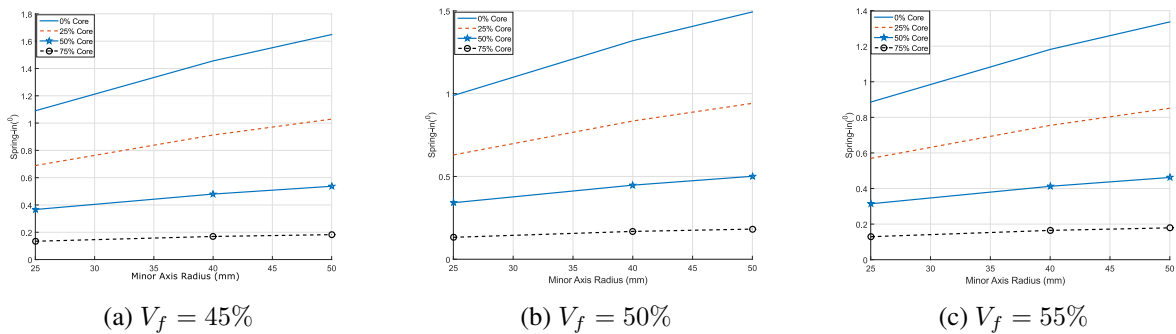


Figure 10: Effect of variation of minor axis on Spring-in

3.3 Effect of Variation of Fibre Volume Fraction

The results shown in Fig. (11) are for various core percentages at various curvatures. They show that as the fiber volume fraction increases, the spring-in angle reduces. The regression models are as written in Eq. (7).

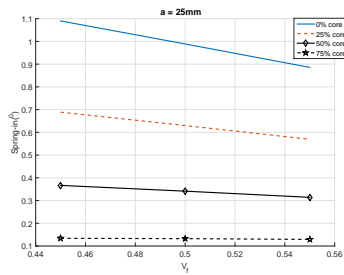
$$\Delta\theta_{a=25mm} = \begin{cases} -2.0435V_f + 2.01 & (0\% \text{ core}) \\ -1.1946V_f + 1.2266 & (25\% \text{ core}) \\ -0.5257V_f + 0.60356 & (50\% \text{ core}) \\ -0.049567V_f + 0.15663 & (75\% \text{ core}) \end{cases} \quad (7a)$$

$$\Delta\theta_{a=40mm} = \begin{cases} -2.7415V_f + 2.6898 & (0\% \text{ core}) \\ -1.5767V_f + 1.6225 & (25\% \text{ core}) \\ -0.67365V_f + 0.78341 & (50\% \text{ core}) \\ -0.046347V_f + 0.19044 & (75\% \text{ core}) \end{cases} \quad (7b)$$

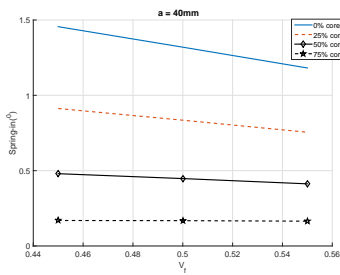
$$\Delta\theta_{a=50mm} = \begin{cases} -3.1218V_f + 3.0538 & (0\% \text{ core}) \\ -1.779V_f + 1.8301 & (25\% \text{ core}) \\ -0.74774V_f + 0.87379 & (50\% \text{ core}) \\ -0.036493V_f + 0.19943 & (75\% \text{ core}) \end{cases} \quad (7c)$$

The regression model for the effect of the fibre volume fraction

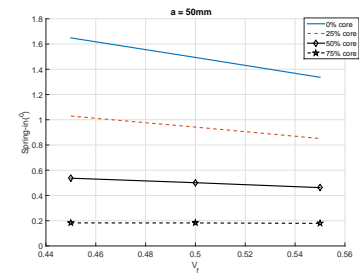
$$\Delta\theta = \begin{cases} 2.0108 - (2.0441 - 3.7786p + 1.4911p^2)V_f + (1.3459p - 3.4827)p & (V_f = 45\%) \\ 2.6907 - (2.7422 - 5.2079p + 2.15p^2)V_f + (1.8973p - 4.7579)p & (V_f = 50\%) \\ 3.0545 - (3.1222 - 6.0095p + 2.5262p^2)V_f + (2.1974p - 5.4558)p & (V_f = 55\%) \end{cases} \quad (8)$$



(a) Minor axis = 25mm

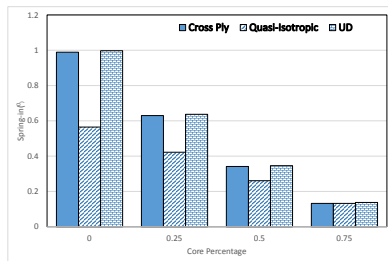


(b) Minor axis = 40mm

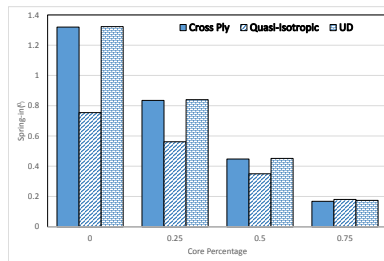


(c) Minor axis = 50mm

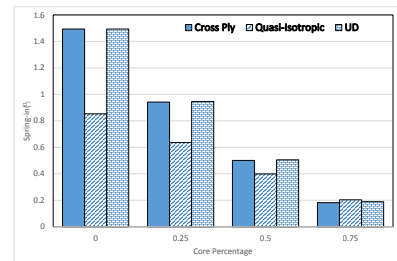
Figure 11: Effect of Fibre Volume Fraction on Spring-in



(a) Minor axis = 25mm



(b) Minor axis = 40mm



(c) Minor axis = 50mm

Figure 12: Effect of Material Layout on Spring-in

3.4 Effect of Stacking sequence

In order to obtain a comprehensive model, a modification coefficient was introduced. By incorporating this coefficient, the model can be used for any stacking sequence. Figure. (12) shows that the spring-in value of the cross ply laminate and

the UD laminate are almost equal while the spring-in value of the quasi-isotropic laminate varies from about 56% at 0% core contribution to about 13% at 75% core contribution. Figure. (13) shows the deformation of some curved panels with different stacking sequence. It was observed that the variation of the spring-in values changed with the core percentage value and not the fibre volume fraction and the curvature of the part. Therefore the charts in Fig. (12) were regressed to obtained Eq. (9) where K is the modification coefficient.

$$K = \begin{cases} 1 & \text{for cross ply and UD laminates} \\ 0.634p + 0.5344 & \text{Quasi-isotropic laminates} \end{cases} \quad (9)$$

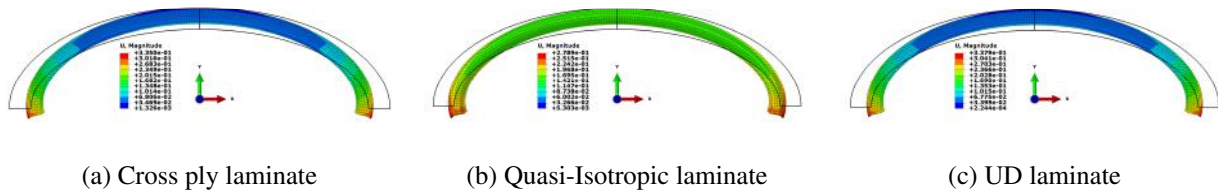


Figure 13: Deformation of curved panels with different material lay-ups

3.5 Overall Regression Model

Thus, the final regression model for the spring-in of E-glass/epoxy curved structures is Eq. (10). The fitted values and original values are compared in Fig. (14). The relative errors are less than 1%.

$$\Delta\theta = K(1.528 + 0.00975a - (1.318 - 2.5p + 1.028p^2)V_f + (0.907p - 0.0122a - 2.553)p) \quad (10)$$

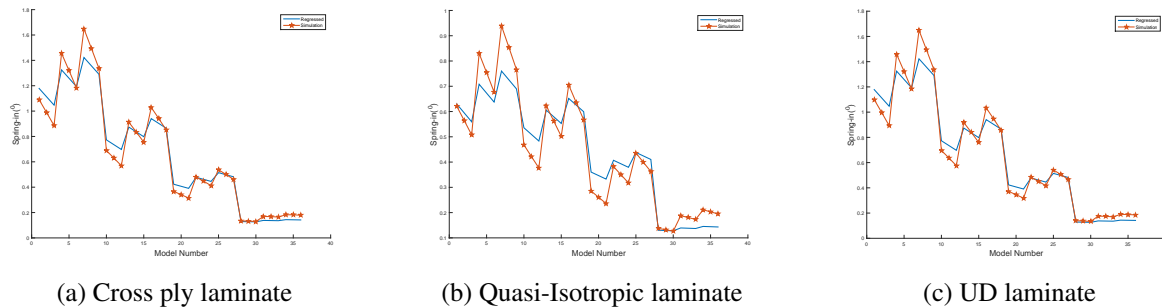


Figure 14: Comparison between fitted values and original values of spring-in for different laminates

4. CONCLUSION

The residual stresses that develop during the manufacture of fibre reinforced composite panels lead to shape distortions, which are also known as spring-in. These distortions are a major source of problems for composite manufacturers. consequently, the ability to effectively and efficiently predict these distortions is always desired. In this paper, a regression-based parametric model was developed. First, process induced shape distortions for various sandwich curved panels was predicted with the aid of the constitutive model originally proposed by Svanberg and Holmberg in ABAQUS. Several factors were varied in the simulations. They include variation in the radius of curvature, stacking sequence (UD, Cross laminate and Quasi isotropic laminate), fibre volume fraction and percentage of core material used. From the results obtained from these simulations, a regression-based parametric model were developed. In order to make the regression model comprehensive, a material modification coefficient was introduced based on statistical analysis of the FEA results. By incorporating this coefficient, the regression-based model can be used to predict the distortions of any of stacking sequence investigated.

The regression-based parametric model can significantly reduce computation time by eliminating the complicated, time-consuming finite element processes and thus provide a quick way of evaluating distortions for curved composite sandwich panels. This model was validated against the FEA solutions. The results show that although there are errors in some cases, the model can predict the dimension variations with relative accuracy.

5. ACKNOWLEDGEMENTS

This work was performed in Instituto Tecnológico de Aeronáutica, Brazil, and was funded by the Nigerian Air Force and CNPq (grants 300886/2013-6 and 301053/2016-2)

6. REFERENCES

- Carolyne Albert and Göran Fernlund. Spring-in and warpage of angled composite laminates. *Composites Science and Technology*, 62(14):1895–1912, 2002.
- Travis A Bogetti, Christopher P Hoppel, and William H Drysdale. Three-dimensional effective property and strength prediction of thick laminated composite media. Technical report, DTIC Document, 1995.
- Hong-Ji Chen and Stephen W Tsai. Three-dimensional effective moduli of symmetric laminates. *Journal of Composite Materials*, 30(8):906–917, 1996.
- Kenan Çınar, Umud Esat Öztürk, Nuri Ersoy, and Michael R Wisnom. Modelling manufacturing deformations in corner sections made of composite materials. *Journal of Composite Materials*, 48(7):799–813, 2014.
- Chensong Dong, Chuck Zhang, Zhiyong Liang, and Ben Wang. Dimension variation prediction for composites with finite element analysis and regression modeling. *Composites Part A: Applied Science and Manufacturing*, 35(6):735 – 746, 2004.
- Nuri Ersoy, Tomasz Garstka, Kevin Potter, Michael R Wisnom, David Porter, and Graeme Stringer. Modelling of the spring-in phenomenon in curved parts made of a thermosetting composite. *Composites Part A: Applied Science and Manufacturing*, 41(3):410–418, 2010.
- G Fernlund, N Rahman, R Courdji, M Bresslauer, A Poursartip, K Willden, and K Nelson. Experimental and numerical study of the effect of cure cycle, tool surface, geometry, and lay-up on the dimensional fidelity of autoclave-processed composite parts. *Composites part A: applied science and manufacturing*, 33(3):341–351, 2002.
- Göran Fernlund. Spring-in of angled sandwich panels. *Composites science and technology*, 65(2):317–323, 2005.
- Andrew Johnston, Reza Vaziri, and Anoush Poursartip. A plane strain model for process-induced deformation of laminated composite structures. *Journal of Composite Materials*, 35(16):1435–1469, 2001.
- Erik Kappel, Daniel Stefaniak, and Göran Fernlund. Predicting process-induced distortions in composite manufacturing—a pheno-numerical simulation strategy. *Composite Structures*, 120:98–106, 2015.
- Autar K Kaw. *Mechanics of composite materials*. CRC press, 2005.
- Yusuf Mahadik and K Potter. Experimental investigation into the thermoelastic spring-in of curved sandwich panels. *Composites Part A: Applied Science and Manufacturing*, 49:68–80, 2013.
- OM Makinde, AR Faria, and MV Donadon. Prediction of shape distortions in angled composite structures. In *Proc. 6th Int. Symposium on Solid Mechanics*, page 302, 2017.
- Abaqus Users Manual. Version 6.10. *ABAQUS Inc*, 2010.
- L Mezeix, A Seman, MNM Nasir, Y Aminanda, A Rivai, B Castanié, P Olivier, and KM Ali. Spring-back simulation of unidirectional carbon/epoxy flat laminate composite manufactured through autoclave process. *Composite Structures*, 124:196–205, 2015.
- DW Radford and TS Rennick. Determination of manufacturing distortion in laminated composite. In *Proc. 11th Int. Conf. Compos. Mater. Compos. Process.: Microstruct Woodhead Publishing*, page 302, 1997.
- DW Radford and TS Rennick. Separating sources of manufacturing distortion in laminated composites. *Journal of Reinforced Plastics and Composites*, 19(8):621–641, 2000.
- J Magnus Svanberg and J Anders Holmberg. Prediction of shape distortions part i. fe-implementation of a path dependent constitutive model. *Composites part A: applied science and manufacturing*, 35(6):711–721, 2004a.
- JM Svanberg and J Anders Holmberg. Prediction of shape distortions. part ii. experimental validation and analysis of boundary conditions. *Composites Part A: Applied Science and Manufacturing*, 35(6):723–734, 2004b.
- JM Svanberg and JA Holmberg. An experimental investigation on mechanisms for manufacturing induced shape distortions in homogeneous and balanced laminates. *Composites Part A: Applied Science and Manufacturing*, 32(6): 827–838, 2001.
- Graham Twigg, Anoush Poursartip, and Göran Fernlund. An experimental method for quantifying tool–part shear interaction during composites processing. *Composites Science and Technology*, 63(13):1985–2002, 2003.

7. RESPONSIBILITY NOTICE

The authors are the only responsible for the printed material included in this paper